Field Strength Prediction by Ray-Tracing for Adaptive Base Station Positioning in Mobile Communication Networks

Thomas Fritsch, Kurt Tutschku and Kenji Leibnitz
Institute of Computer Science, University of Würzburg
Am Hubland, D-97074 Würzburg, Germany

Abstract: *The Adaptive Base Station Positioning Algorithm (ABPA) is presented, which is based on a neural net approximation of the traffic density in the coverage area of a cellular mobile communication system. ABPA employs simulated annealing, thereby achieving quasi-optimal base station locations depending on the topography of the investigated area. Furthermore, ABPA considers the radio wave propagation within this area for the base station positions. Therefore, a three dimensional digital surface model is used to approximate the topography and two field strength prediction methods, a line-of-sight (LOS) approach and a ray-tracing technique, are investigated within the context of adaptive positioning. In particular, the results obtained by the ray-tracing technique are encouraging, showing supplying areas, which seem to be similar to those, stemming from real measurements. However, as simulations show, the more realistic field strength prediction by ray-tracing has a strong influence on the performance of ABPA, resulting in different base station locations. As an outlook, the combination of field strength prediction using ray-tracing with adaptive traffic prediction on a road graph by neural nets is proposed for further investigation.*

1   Introduction

The growth of the mobile cellular market imposes a difficult task to the designers of mobile communication systems. The determination of the base station locations depends mainly on two factors: a) the inhomogeneously distributed user density in the coverage area of the base stations, e.g. a location area in the GSM system, and b) the varying radio signal strength. When a mobile unit is moving through the supplying area of a base station, it receives a time-varying radio signal due to reflections, shadowing on obstacles and diffusion by scattering. In the planning process, the disturbances of the radio signal caused by these physical phenomena are usually considered by rough estimations of the field strength models using statistical assumptions [7]. Another method is the approximation of the field strength level with models developed in the context of geometrical optics [9]. However, the latter models require an extremely high computing effort. Moreover, since the mobile subscribers move through the cellular network along traffic highways, the resulting mobile teletraffic density depends both on geographical location and on time. Consequently, the mobile teletraffic distribution can be decomposed in two parts, the one concerning the *average local* distribution of mobile user density in a coverage area, the other representing the *time-varying* component due to traffic mobility caused by working hours, car traffic behavior, etc. The planning of adequate base station positions has to consider the first
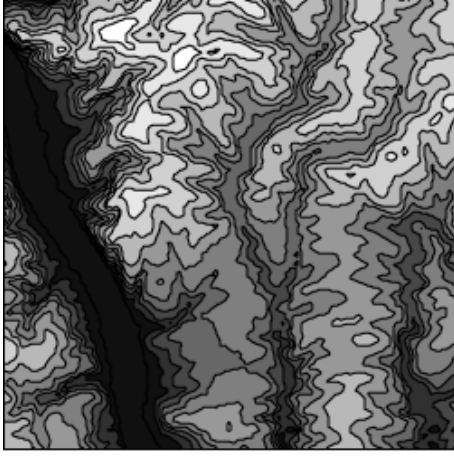
part, whereas the second can be tackled by dynamic frequency assignment or network restructuring methods.

In this paper we focus on the problem of finding optimal positions of base stations, whose supplying areas are covering the regions where the teletraffic takes place. An adaptive base station positioning algorithm (ABPA), using a set of formal neurons, distributed according to the estimated local user density, was presented in [6]. In Section 2 we present a short outline of ABPA. This algorithm is already able to provide a meaningful solution of the base station positioning problem, but the field strength prediction method used by ABPA can essentially be improved, since its approximation quality was kept low to avoid extensive computations. In Section 3 of this paper, free space propagation of radio waves is shortly reviewed and the Line-of-Sight (LOS) approach used so far in ABPA is described. Furthermore, the concept of field strength approximation using ray-tracing techniques in combination with ABPA is discussed. In Section 4 we present first results of ABPA using this modification. The improvement of ABPA will facilitate solutions of the base station positioning problem, which take realistic topographical scenarios into account. As a future task, the combination of ray-tracing based field strength prediction methods with a modification of selforganizing feature maps, the Neural Gas algorithm, is proposed in Section 5. This combination is supposed to tackle more accurately the problem of adapting the local average traffic density in the context of ABPA.
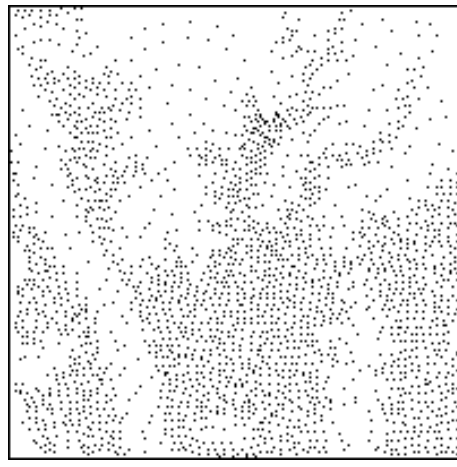
2   Outline of ABPA Using Selforganizing Feature Maps

The **A**daptive **B**ase Station **P**ositioning **A**lgorithm, presented in [5, 6], is based on the idea that competing base stations try to maximize their supplying areas by covering a maximum number of sensory objects, called sensory neurons. These neurons are distributed in the terrain, to be supplied with radio frequencies, according to a given density, which stems from the learning process of a selforganizing neural net. This density is assumed to be an estimation of the local teletraffic density, since it is more likely that car traffic and thereby mobile telephony takes place at data points of *low* terrain than at data points of *high* terrain. A selforganizing feature map was used to adapt the low terrain data of the digital terrain model of the topography, depicted in **Figure 1(a)**. In **Figure 1(b)** the result of the adaptation process is illustrated. The geographical topography, which was investigated, represents the area north-west of Würzburg. Selforganizing feature maps (SOM) are preserving the topology of the input vector space by adapting their weight structure accordingly. The reader is referred to [8] for a detailed description of SOMs.

The usage of neurons by ABPA in the prestructuring step provides a set of sensory elements for the field strength level. In the algorithm, the supplying areas of the base stations, described by their location, transmitting power and a positioning error, are determined. Hereby the comparison of the received field strength level with a given threshold at the neuron positions is taken as the criterion, whether a neuron belongs to a base station supplying area or not. Each new arrangement of base stations is denoted as an adaptation step of the algorithm. Each base station can change its position or its transmitting power, thereby achieving different supplying areas. The positioning error of the base stations is a measure for a reasonable choice of their current locations, *before* the actual adaptation of these locations takes place. In this step, the base station with the worst positioning error is moved into the direction where clusters of attracting sensory neurons are located or into

(a) Digital Terrain Model

(b) Selforganizing feature map

Figure 1: Neural approximation of the digital terrain model

the direction which is resulting from the repellation of other base stations located in the immediate surrounding of the base station considered. The determination of supplying areas afterwards implies the field strength prediction for all neurons in the coverage area according to the methods described in detail in Section 3.

In the course of ABPA, each complete adaptation step is followed by a system state evaluation, which is embedded in a *simulated annealing* process [1]. A system state Z at time step t is characterized by the assignment of all sensory neurons S_i depending on the current distribution of the transmitting stations T_j and their corresponding supplying areas $V(T_j)$ to one of the following sets:

1. free sensory neurons $\mathbf{S_f} := \{S_i | S_i \notin \mathbf{V}\}$

2. multiply assigned sensory neurons
   $\mathbf{S_m} := \{S_i | S_i \in \bigcup_{l,j} \{V(T_j) \cap V(T_l)\}\}, \forall l, \ \forall j, \ l \neq j$

3. definitely assigned sensory neurons $\overline{(\mathbf{S_f} \cup \mathbf{S_m})}$

A system state is associated with a system energy, which is proportional to the magnitude of $(\mathbf{S_f} \cup \mathbf{S_m})$. A minimization of the system energy corresponds to the maximization of the definitely assigned neurons. Thus, an optimal coverage of the terrain can be obtained. However, such a result can only be achieved if the simulated annealing procedure [1] is used to govern the system state transitions. Hereby each state transition takes place with probability:

$$P\{Z^{(new)} = Z^{(cur)}\} = e^{-\frac{\Delta E}{\tau}}. \tag{1}$$

This implies, that the current system state $Z^{(cur)}$ is accepted as a new system state $Z^{(new)}$ according to the expression on the right hand side of eqn. (1). The decreasing temperature τ plays the role of a cooling parameter of the system and is introduced to prevent the system of getting stuck in local minima of the energy function landscape. A final stationary state, representing the suboptimal locations of base stations, is reached, if τ declines to zero.

The accuracy of ABPA depends on the determination of the field strength level at the neuron positions, as well as on an appropriate distribution of the neurons itself. An improvement of ABPA concerns the restriction of the neuron positions to road and highway locations in the coverage area and is proposed in Section 5.

3   Field Strength Approximation in the Supplying Area

A key issue in mobile system planning as well as in ABPA is the prediction of field strength in the investigated supplying area. The received signal depends mainly on two environmental factors: a) the *topographical* structure and b) the *morphographical* properties of the area. These factors determine the influence of three basic radio propagation phenomena: diffraction, reflection and scattering. *Diffraction* is mainly governed by the topographical structure and occurs, when the direct radio path between transmitter and receiver is obstructed by natural (e.g. hills) or human-made objects (e.g. buildings). Based on Huygen's principle, secondary waves are formed behind the object, even if there is no line of sight between transmitter and receiver. Thus a radio signal can be received in the "shadow" of an object. *Reflections* are observed, when a radio wave strikes an object which is very large, comparing to the wave length. The reflection coefficients vary for different surfaces of objects. *Scattering* occurs when the radio path contains objects with dimensions that are in the order of the wave length (e.g. leafs of trees). Since scattering is based on the same mechanism as reflection, it causes the energy of the radio beam to be reradiated diffusely. The strength of reflection and scattering is substantially influenced by morphographical properties.

In the literature, a lot of models for radio wave propagation are proposed [2, 7, 9]. Complex proposals provide a good approximation of the path loss, but require high computational effort. Simple models require less computational power, but estimate the field strength only roughly. Within ABPA, the field strength prediction takes place in each adaptation step. Therefore, the applied field strength prediction method has to show a good trade-off between computation requirements and approximation accuracy. After a short outline of path loss within free space propagation, the line-of-sight (LOS) approach used by ABPA is described in subsection 3.2.

3.1   Characterization of Path Loss within Free Space Propagation

A detailed description of the free space propagation model can be found in [3, 7]. For this model, it is assumed that no obstruction disturbs the propagation of the radio wave. The signal strength in the supplying area is characterized by the electromagnetic field strength of the received wave. Since in free space waves are propagating equally in each direction, the wavefront has the form of a a sphere. Therefore the power density S_r at the receiver in distance d is:

$$S_r = P_t G_t / A_{\mathrm{sphere}} = P_t G_t / (4\pi d^2). \tag{2}$$

Hereby P_t denotes the transmitting power and G_t the antenna gain. The product $P_t \cdot G_t$ is called *equivalent isotropically radiated power (EIRP)* considering the fact, that only

antennas, emitting waves of equal strength in each direction, are taken into account. The field strength E_r at the receiver is:

$$E_r = \sqrt{S_r Z_0} = \sqrt{30 G_t (P_t/W)}/(d/m) V/m, \tag{3}$$

where $Z_0 = 120\pi\ \Omega$ denotes the wave resistance for vacuum. The field strength level e_r at the receiver is defined as:

$$\begin{aligned} e_r/(db(\mu V/m)) &= 20\lg(E_r/(\mu V/m)) \\ &= 74,8 + 10\lg(P_t/W) + 10\lg(G_t) - 20\lg(d/km). \end{aligned} \tag{4}$$

In general, the signal loss is equivalent to the ratio between the transmitted and the received power, which is calculated in logarithmic scale. Regarding A_{eff} as the effective absorption cross section of an antenna and G_r as the antenna gain, the received power P_r results to:

$$P_r = S_r A_{\text{eff}} = S_r G_r \lambda^2/4\pi = E_r^2 \lambda^2 G_r/(4\pi Z_0) \quad \text{with} \quad A_{\text{eff}} = G_r \lambda^2/4\pi. \tag{5}$$

Thus, regarding the path loss level L_{P}, the following applies:

$$L_{\text{P}}(db) = 10\lg(P_t/P_r) = 10\lg P_t - 20\lg E_r - 10\lg\frac{\lambda^2}{4\pi} + 10\lg Z_0. \tag{6}$$

From eqn. (6) follows that the path loss only depends on the transmitting power and the field strength. In case of free space propagation, eqn. (6) can be simplified to:

$$L_0 = 32.5 + 20\lg(d/km) + 20\lg(f/MHz) - g_t/dBi - g_r/dBi, \tag{7}$$

where f is the frequency of the radio signal and g_r and g_t denote the logarithmic measure of the antenna gain. Eqn. (7) provides a simple formula to compute the free space path loss, which only considers the distance between receiver and transmitter. Hata [7], extended the free space propagation model regarding morphographical properties. More generally, an additional parameter n is used, describing the relationship between distance and received power:

$$L(d) = L(d_0) + 10\,n\,\lg(d/d_0) + X_\sigma, \tag{8}$$

where X_σ is a zero-mean Gaussian random variable, that represents the variation in average received power, and d_0 denotes a reference distance. The parameter n varies for different signal environments [2]. In eqn. (5) the value of n is 2, denoting the exponent of E_r.

3.2   Line-of-Sight (LOS) Approach

In ABPA, the field strength level is calculated according to eqn. (4), which was modified to take the path loss, caused by diffraction, into account. In **Figure 2** a typical scenario is depicted. A mountain is obstructing the direct propagation of the radio wave from the transmitter to the mobile station. Due to diffraction, occurring at the top of the hill, the radio signal can also be received in the shadow of the mountain. In the LOS approach the actual distance as well as the amount of the obstructed radio path is considered. The field strength level at the mobile station is approximated by:

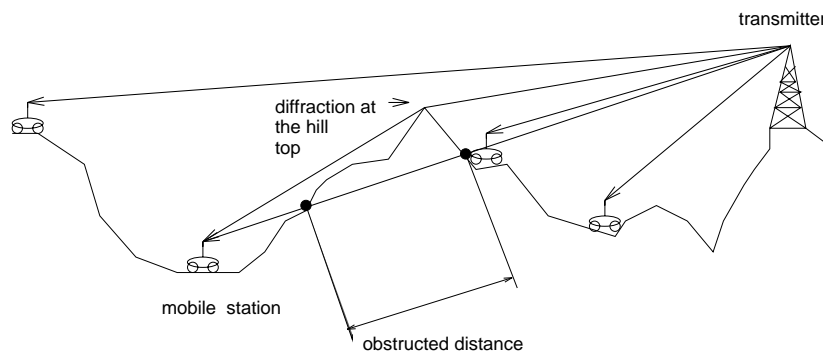$$e_r' / (db(\mu V/m)) = e_r - \rho_S \cdot d_{\text{obstruct}} / (db(\mu V/m)), \tag{9}$$

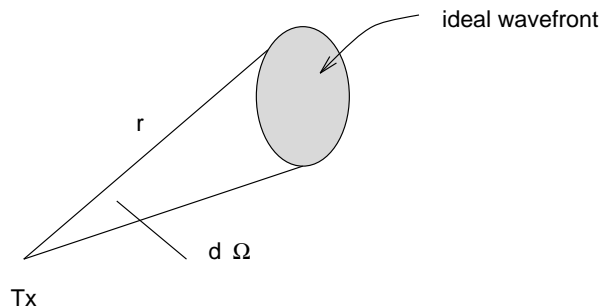**Figure 2**: Modeling the shadowing effect

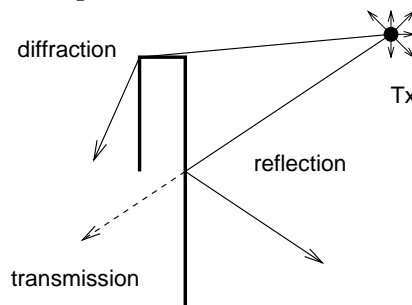**Figure 3**: Ideal wavefront represented by each source ray
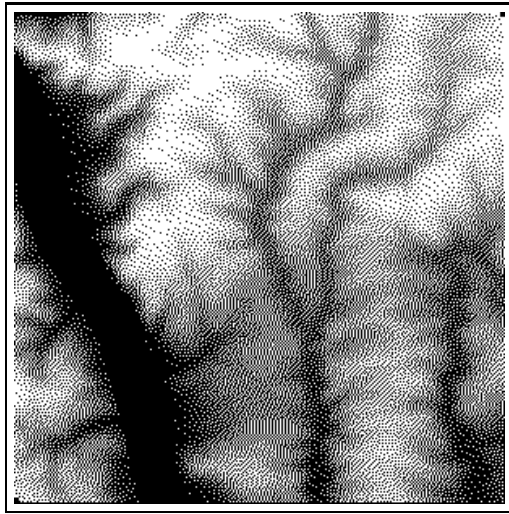

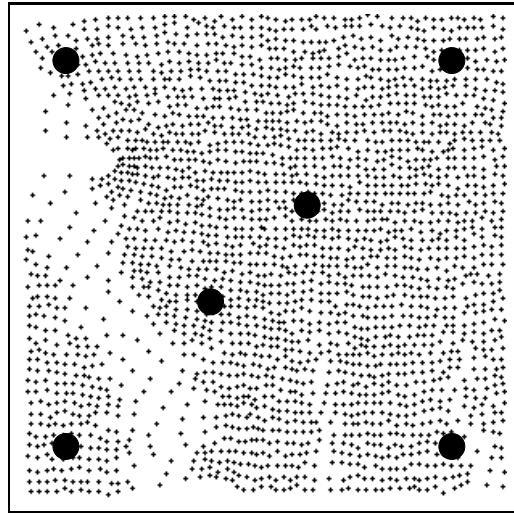**Figure 4**: Diffracted and reflected rays from transmitter Tx

where ρ_S is a proportional factor. The obstructed distance d_{obstruct} can effectively be computed using *Bresenham's* line algorithm [4]. For rural environment, the heuristic assumption made above is quite useful since the diffraction effects are not very strong in this case. In urban regions the distances from transmitters to the obstructing objects are usually smaller and thus diffraction has higher impact. As a consequence, the LOS approach fails for urban environment.

3.3   Field Strength Approximation Using Ray-Tracing

Originally, ray-tracing techniques have been introduced in computer graphics applications to create photorealistic pictures of 3D sceneries [12]. Ray-tracing algorithms are able to visualize accurately optical effects like shadowing, transparency, etc. This capability makes the method attractive for field strength predictions [11]. Ray-tracing is based on the light house idea. Radio beams are emitted from a transmitter Tx in distinct directions. The beams "illuminate" the scenery, i.e. the supplying area. In the algorithm, the beams are modeled as ray tubes with the fixed solid angle $d\Omega$ and of identical shape and size in distance r from the transmitter, cf. **Figure 3**. The path of an individual beam is traced recursively until it strikes an object, cf. **Figure 4**. If a ray strikes an edge or the surface of the digital terrain model, diffraction or reflection of the ray takes place. Reflection can be modelled very easily using the *Fresnel* equations [13]. For diffraction, *Huygen's* principle in conjunction with the *Kirchoff* laws has to be used to compute the decline in energy of the ray. Since ray-tracing tracks each beam individually, the behavior of the ray can be traced in detail at the cost of increased computing effort. An remaining problem, using ray-tracing, is the determination of the correct beam width $d\Omega$, i.e. the number of emitted rays, to achieve a certain approximation accuracy.
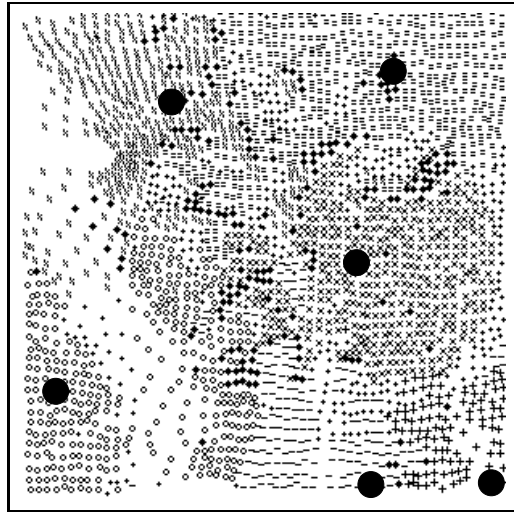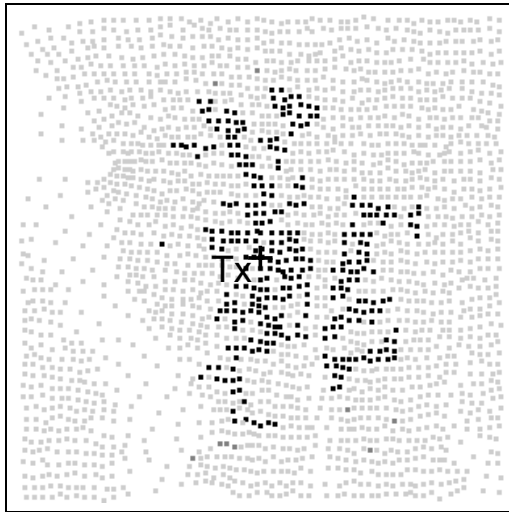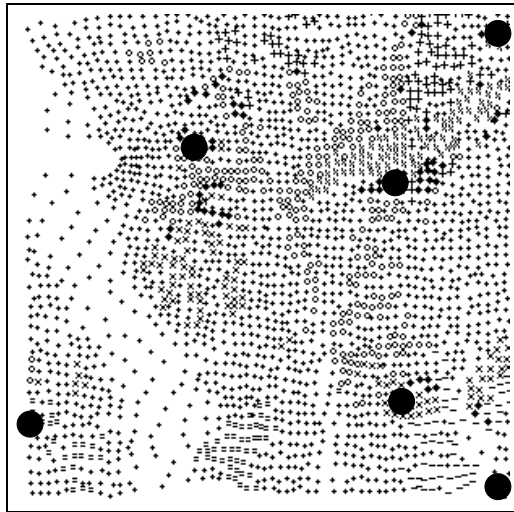
Figure 5: The 3D terrain model (a) and the supplying areas for (b) LOS and (c) ray-tracing

Figure 6: Initial configuration (a) of ABPA and the base station locations obtained by (b) LOS and (c) ray-tracing

3.4 Supplying Areas

Using the two field strength approximation methods described above, simulations with a single transmitter for a real supplying area have been carried out. The investigated terrain is again the $10km \times 10km$ area in the north-west of the city of Würzburg, cf. **Figure 5(a)**. The city center is located in the lower part of the picture and on the left side the river Main is visible. The hilly topography of this area can be considered typical for central Europe. The 3D model of this area consists of altitude values, sampled every 100 meters, and the surface is interpolated by triangles using the altitude points as vertices. The sensory neurons are distributed according to the prestructuring step of ABPA, cp. Section 2. The transmitter Tx in **Figure 5(b)** and **Figure 5(c)** is located in the center of each picture and the neurons, receiving a field strength level above a certain threshold, are marked by bold print. These neurons form the "supplying area" of the transmitter. The approximation of this area using the LOS approach is depicted in **Figure 5(b)**. Here, eqn. (4) and eqn. (9) have been applied to compute the field strength level. The connectivity of the supplying area is very high, whereas for the ray-tracing approach, cf. **Figure 5(c)**, the "lacunarity" of this area is high. In the latter case, reflection were followed until depth one, using a reflection coefficient of 1.0. The signal level was obtained by eqn. (4) with the total traversed path length as the distance d. The large "holes" in the supplying area indicate that the path loss is greater, than predicted by the LOS approach. As shown in Section 4, this will effect the ABPA substantially.

4 Finding Optimal Base Station Locations

To prove the capability of ABPA and the two field strength prediction techniques discussed in this paper, ABPA was tested on the topography north-west of Würzburg. The algorithm was used to find the best locations of six transmitters in this terrain. The initial configuration of the transmitter and the sensory neurons is depicted in **Figure 6(a)**. **Figures 6(b)** and **(c)** show the base station locations, obtained by using the LOS approximation and the ray-tracing prediction, respectively. The transmitters are marked by ● and the different supplying areas for the individual transmitters are tagged by various symbols. The ABPA using LOS (cf. **Figure 6(b)**) achieved a very good coverage of the supplying area: 77% of the sensory neurons are definitely assigned, 19% of the neurons are not assigned (marked by a ·) and 4% are supplied by at least two base stations (marked by ◆). The locations of the base stations are fairly regularly distributed over the terrain. The result of ABPA in conjunction with ray-tracing is depicted in **Figure 6(c)**. In this case the algorithm achieved only a poor coverage: 29% of the sensory neurons are definitely assigned, 68% of the neurons are not assigned and 3% are multiply supplied. Two transmitters are placed on dominant positions in the central part of the picture. The others are placed at the margins of the investigated area. Since the supplying areas of the individual transmitters don't overlap very much, the transmitters located in the center increase their sphere of influence and force the other base stations to cover only the marginal areas.
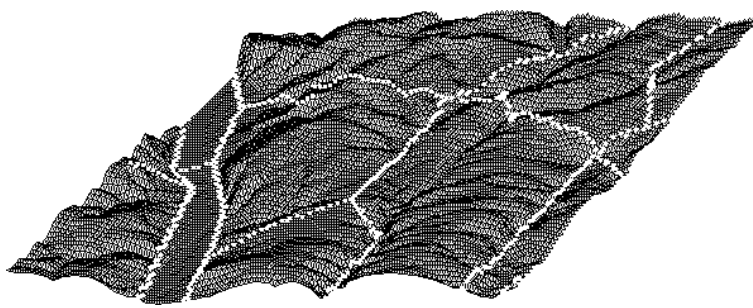
Figure 7: Neural approximation of the road graph in coverage area

5 Outlook

A possible extension of the ABPA to increase the accuracy of the algorithm consists of using a different distribution of the sensory neurons. Instead of approximating low terrain data by a selforganizing feature map, as described in Section 2, the neurons can be distributed on a road graph of the coverage area using a variant of the original SOM algorithm, the so-called *Neural Gas* [10]. The neurons behave analogously to particles of a gas and can therefore adapt readily any probability distribution. A special feature of this algorithm is its ability to approximate subspaces of varying dimensions and preserving its topologies. If measurements of mobile car traffic are available, this data can be used to estimate the local average teletraffic density along the road graph. As a result of the Neural Gas learning process, the neurons will distribute themselves inhomogeneously on the road graph according to the measured vehicle traffic density. The approximation of the road graph using the Neural Gas algorithm is depicted in **Figure 7**. Hereby the adaptation of the traffic density has not yet been implemented and therefore the neurons are spaced equally on the road graph. Due to the different distribution of the neurons ABPA is expected to locate the base stations in accordance to the actual teletraffic.

6 Conclusions

We presented a neural net approach for the adaptive positioning of base stations (ABPA) in a cellular mobile communication system using an LOS and a ray-tracing technique for field strength approximation. The obtained results are encouraging, since ABPA can also be used, when the radio wave propagation is modelled by ray-tracing in a more realistic way. Although ABPA using ray-tracing does not achieve the same high coverage as with LOS, the algorithm has the ability to find suboptimal base station locations. Some extensions to avoid the driving out of some base station to the margins should be implemented. We expect that the approach presented in this paper will provide a powerful tool for planning cellular mobile communication networks.

References

[1] E. Aarts and J. Korst. *Simulated Annealing and Boltzmann Machines*. John Wiley & Sons, Chichester, 1990.

[2] J. B. Andersen, T. S. Rappaport, and S. Yoshida. Propagation messurements and models for wireless communications channels. *IEEE Communications Magazine*, 33(1):42–49, 1995.

[3] H. Bürkle, editor. *Grundlagen der Funktechnik*, volume 13 of *TTKom*. R.v.Decker's Verlag, Heidelberg, 1989.

[4] J. Foley and A. Van Dam. *Fundamentals of Computer Graphics*. Addison-Wesley, 1983.

[5] T. Fritsch. *Neural Nets in Planning and Optimisation of Mobile Communication Systems (in German)*. PhD thesis, Universität Würzburg, Lehrstuhl f. Informatik III, 1995.

[6] T. Fritsch and S. Hanshans. An integrated approach to cellular mobile communication planning using traffic data prestructured by a self-organizing feature map. In *Proceedings of the 1993 International Conference on Neural Networks*, pages 822D–822I. IEEE, IEEE Service Center, M"arz 28 – April 1 1993.

[7] M. Hata. Empirical formula for propagation loss in land mobile radio services. *IEEE Transactions on Vehicular Technology*, 29(3):317–325, August 1980.

[8] T. Kohonen. *Self-Organizing Maps*, volume 30 of *Springer Series in Information Sciences*. Springer-Verlag, Berlin, 1995.

[9] T. Kürner, D. J. Cichon, and W. Wiesbeck. Concepts and results for 3D digital terrain-based wave propagation models: An overview. *IEEE Journal on Selected Areas in Communications*, 11(7):1002–1012, September 1993.

[10] T. Martinetz and K. Schulten. Topology representing networks. *Neural Networks*, 7(3):507–522, 1994.

[11] J. McKown and R. Hamilton. Ray tracing as a design tool for radio networks. *IEEE Network Magazine*, 5(6), November 1991.

[12] T. Whitted. An improved illumination model for shaded display. *Communications of the ACM*, 23(6):343–349, 1980.

[13] H. Zinke O.; Brunswig. *Lehrbuch der Hochfrequenztechnik*, volume 1. Springer-Verlag, Berlin, 4 edition, 1990.